WILEY | Hindawi

Research Article

Seismic Sedimentologic Study on Sequence-Sediment Evolution in Fault Basin Regions

Wang Tianyun [iD],[1,2] **Tian Jingchun,**[1] **Liu Wei,**[2] **Han Xiaofeng,**[3] **Li Yuan,**[2] **Li Tao,**[2] **and Sun Xiaoping**[2]

[1]*Institute of Sedimentary Geology, Chengdu University of Technology, Chengdu, Sichuan 610059, China*
[2]*BGP, CNPC, Zhuozhou, Hebei 072751, China*
[3]*Xi'an Geological Survey Center, China Geological Survey Bureau, Xi'an, Shanxi 710000, China*

Correspondence should be addressed to Wang Tianyun; wangtianyun03@cnpc.com.cn

With potential hydrocarbon source rocks, the Mesozoic Lower Cretaceous interval in the Aitegle Sag of the Yingen-Ejinaqi Basin in China has a bright petroleum exploration prospect. Considering the scarcity of wells in Aitegle Sag, we have systematically carried out the research on the sequence structure and sedimentary system evolution of the Lower Cretaceous based on seismic, core, and logging data, guided by the Vail classic sequence stratigraphy, and innovatively introduced the self-organizing mapping neural network (SOM) learning algorithm to assist in seismic geological analysis. The results are as follows: (1) after RMSAmp, LyapIndex, FrctDim, and InfoEntr clustering, five zones are divided, which are corresponding to five seismic facies (showing medium-strong amplitude and parallel-subparallel reflection; medium-strong amplitude and wedge-shaped divergent reflection; medium-strong amplitude and continuous-relatively continuous, parallel-subparallel reflection; strong amplitude and continuous sheet-like or blank reflection; and weak amplitude and mound-shaped chaotic reflection, respectively), and interpreted as five subfacies including delta plain front, prodelta-shallow lake, semideep lake, deep lake, and sublacustrine fan. (2) The Lower Cretaceous formation includes one second-order sequence, three third-order sequences (SQ2–SQ4), and six system tracts. In the SQ2–SQ4 circle, the delta system formed by sediments from southeast varies remarkably in the progradational zones in different system tracts, and tectonic movements and sediment supply control the sequence stratigraphy in the study area as major factors. (3) It is feasible to apply SOM learning algorithm to seismic attribute clustering analysis. This method effectively realizes the combination of geophysical methods based on big data analysis and geological problem analysis, which not only strengthens the use of seismic data but also ensures the effectiveness and reliability of clustering results. These findings offer basic data and scientific supports for the exploration and development of unconventional reservoirs (e.g., shale and tight oil/gas reservoirs) in the Aitegle Sag and also provide new ideas for studying the sequence-sediment in the target zones in the fault basin regions with scarce wells.

1. Introduction

The Yingen-Ejinaqi Basin is a large petroliferous basin in China, where exploration was dated to the 1950s. Except for a small-medium-sized oilfield in the Chagan Sag to the east, no breakthrough has been made in the basin [1–7]. Since 2000, with the advancement of exploration and development technologies for unconventional oil and gas, high-yield oil and gas flows have been obtained from the Lower Cretaceous limy shale reservoirs in the Hari Sag of the Suhongtu Depression, revealing a favorable prospect of unconventional oil and gas exploration [8–12].

Adjacent to the Hari Sag, the Aitegle Sag is a new potential exploration target, but its sequence stratigraphic and sedimentary characteristics have not been investigated sufficiently. In contrast, the Hari Sag has been highly explored and analyzed systematically on its structure, sequence-sediment, reservoirs, and petroleum geochemical features. The

Hari Sag mainly contains such sedimentary facies as alluvial fan, fluvial, delta, and lacustrine facies [13, 14]. In the Suhongtu Formation and the Bayingobi Formation, major hydrocarbon source rocks are generally characterized by the coexistence of various unconventional and conventional reservoirs that are composed of limy shale, sandstone, and volcanic rock [12, 14–20]. After pores and throats in these reservoirs were recognized, the limy shale reservoir was classified into a kind of reservoir with ultralow porosity and ultralow permeability [21–25].

Aitegle Sag is controlled by a synsedimentary fault at the boundary and is a typical fault-depressed basin with few wells. Although many scholars have carried out sequence-sedimentary studies on different fault-depressed basins, there are few studies on the sequence-sedimentary coupling relationship in fault-depressed basins with few wells. How to effectively improve the reliability of research results is the focus and difficulty of this study.

This study fully relies on geological and geophysical data to establish the Mesozoic Lower Cretaceous sequence stratigraphic division scheme in Aitegle Sag. In the study of seismic facies, we innovatively introduced the self-organizing mapping neural network analysis technology into the process of seismic geology research, combined the unsupervised self-organizing neural network learning algorithm with the seismic attribute clustering analysis process, and effectively realized the combination of geophysical methods based on massive data analysis and geological problem analysis. This study is of great significance for guiding the sequence-sedimentary study in fault basin regions with scarce wells.

The study results provide new ideas for investigating the sequence-sediment in the target zones in the fault basin regions with scarce wells and suggest the future direction of unconventional oil and gas exploration.

2. Geological Setting

The Yingen-Ejinaqi Basin in North China spans four tectonic units (i.e., Tarim, Kazakhstan, Inner Mongolia-Northeast China, and North China) which are different in properties (Figures 1(a) and 1(b)). The Aitegle Sag, namely, the study area, is located in the central-east of the Suhongtu Depression at the central-northern margin of the Yingen-Ejinaqi Basin and covers a total area of nearly 2,000 km^2.

2.1. Structural Characteristics. The Yingen-Ejinaqi Basin is a Paleozoic-Mesozoic superimposed inland basin in China. It is composed of multiple unequal-sized small fault lake basins developed during the Mesozoic period (Figure 1(c)). The Suhongtu Depression at the central-northern margin presents a structural pattern with alternating uplifts and sags (Figure 1(d)). Boundary faults in all the sags are sedimentation-controlled growth faults and experienced similar tectonic-sedimentary evolution processes [6, 26]. The Aitegle Sag is close to the Aogao Uplift (an alpine zone) in the northwest and separated from the Maima Sag by a small uplift (a hilly zone) in the southeast (Figure 1(e)).

The Aitegle Sag was a sea-land in the Carboniferous-Permian and then developed into an intracontinental lake basin in the Mesozoic.

In the Carboniferous-Permian, the Caledonian-early Variscan tectonic zone was extensively active, the structural rudiment of a basin was basically formed, and multistage volcanic eruptions and plutonic intrusive rocks were developed extensively. Littoral-neritic deposits were dominant and developed into pyroclastic rock and clastic rock interbedded with coal seams.

A long-term uplifting induced by the Indosinian movement resulted in the absence of Triassic and Jurassic strata and a large angular unconformity between the Carboniferous-Permian and the overlying Cretaceous. In the Cretaceous, namely, the basin-mountain transformation stage, the sags subsided and accepted sediments again.

It is believed that the Cretaceous was the major period during which the Mesozoic strata developed in the Yingen-Ejinaqi Basin, and it is also the key depositional period worthy of attention in exploration and development. During the period, episodes III–V of the Yanshanian movement were influential and specifically controlled the fault-depression transformation and sag deposition. Driven by multistage tectonic movements, structurally, the Aitegle Sag presents as a single-fault lake basin [2, 3, 6, 27].

2.2. Sedimentary Environment. In the Cretaceous, as the lake water level dropped, the grain sizes of sediments gradually increased in the Aitegle Sag. A transition from lacustrine facies to delta facies and fluvial facies occurred, forming the Lower Cretaceous strata successively. The Lower Cretaceous has widely distributed lacustrine source rocks, favorable reservoir-caprock assemblages, and both unconventional and conventional oil and gas reservoirs [1, 2, 28].

The Bayingobi Formation is dominated by lacustrine deposits and composed of a mottled conglomerate interval with inequigranular sandstone in the lower part, grey limy mudstone with siltstone in the middle part, and lime-bearing mudstone in the upper part. The Suhongtu Formation is dominated by lacustrine and delta deposits and composed of grey mudstone with siltstone in the lower part and fine, grey, pebbly sandstone with mudstone in the upper part. The Yingen Formation is dominated by delta deposits which are mainly mudstone and siltstone [6, 29] (Figure 2).

3. Basic Data and Research Methods

3.1. Basic Data. The Lower Cretaceous interval which is the major exploration target has clear seismic reflections, high SNR (signal-to-noise ratio), accurate restoration of faults, and obvious geological phenomena. The dominant frequency and frequency width are 35 Hz and 40 Hz, respectively (Figure 3). Two exploration wells were drilled into the Lower Cretaceous in the study area, and the basic well and seismic data are qualified for sequence-sediment research.

3.2. Research Idea and Theoretical Methods

3.2.1. Research Idea. The study area is a new exploration area where a four-order sequence classification was made
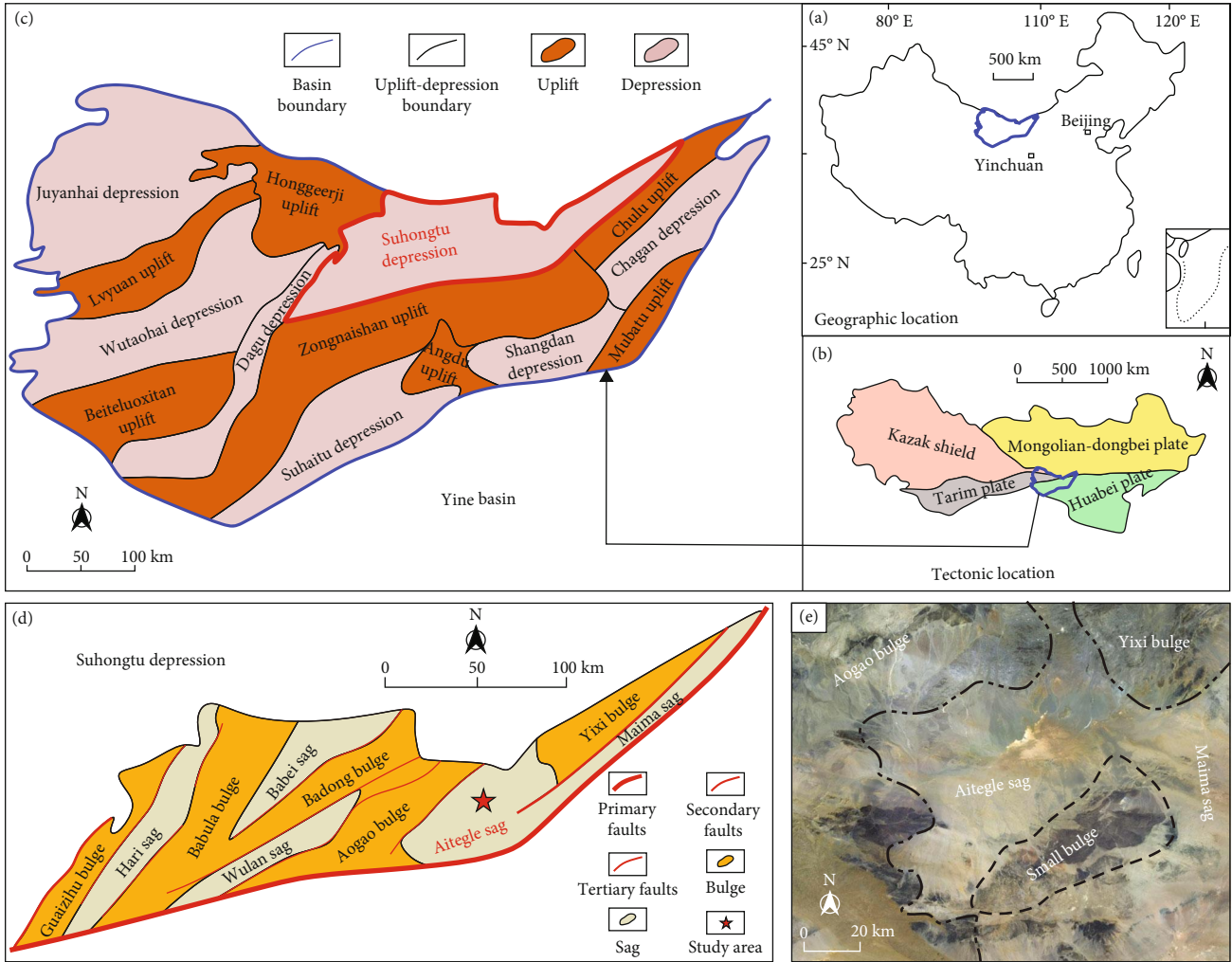
FIGURE 1: Regional structure location map of Aitegle Sag. (a) Regional geographic location of Yin'e Basin. (b) Location relationship between Yin'e Basin and regional plate. (c) Structural zones of Yin'e Basin. (d) Structural zones of Suhongtu Depression and location of Aitegle Sag. (e) Satellite map of Aitegle Sag and surrounding structures.

according to the classical theory of sequence stratigraphy and considering the actual seismic frequency [30–34]. First, based on core, logging, and seismic data, the sequence boundaries are identified, and the isochronous sequence stratigraphic framework is established for the target formation. Then, a set of seismic attributes that can reflect the structural variation within system tracts are selected for self-organizing map (SOM) analysis to map the relationship between seismic facies and sedimentary facies. Finally, the sequence-sediment evolution in the new exploration area with scarce wells is recognized effectively.

3.2.2. SOM Analysis.
Self-organizing map (SOM) is an unsupervised neural network learning technique that allows automatic clustering of input data. The SOM model consists of an input layer and an output layer which are connected by a weighting value. All input neurons are connected to output neurons. Within the input layer, every neuron is connected with eight neighboring neurons, except for marginal ones [35–39] (Figure 4).

Given an input neuron x and an output neuron y, the input signal of y is I_y, the connection weight between x and y is W_{xy}, and I_y is equal to the sum of H_x multiplying the associated W_{xy}.

$$I_y = \sum_{x=1}^{n} W_{xy} H_x. \tag{1}$$

Output neurons are random at the very beginning. Over time, output neurons begin to interact with each other laterally and accumulate into "bubbles," each of which is centered by a specific neuron A (a winning node). A "bubble" refers to a subset of neurons N_A within a certain radius. In the case that an output neuron y both belongs to N_A and does not belongs to N_A, during training, N_A monotonically decreases centering on A and finally terminates at A. All the weights for neurons within the scope have to be adjusted for successive approximation to input signals. As the earning rate δ increases and gradually approaches to zero,
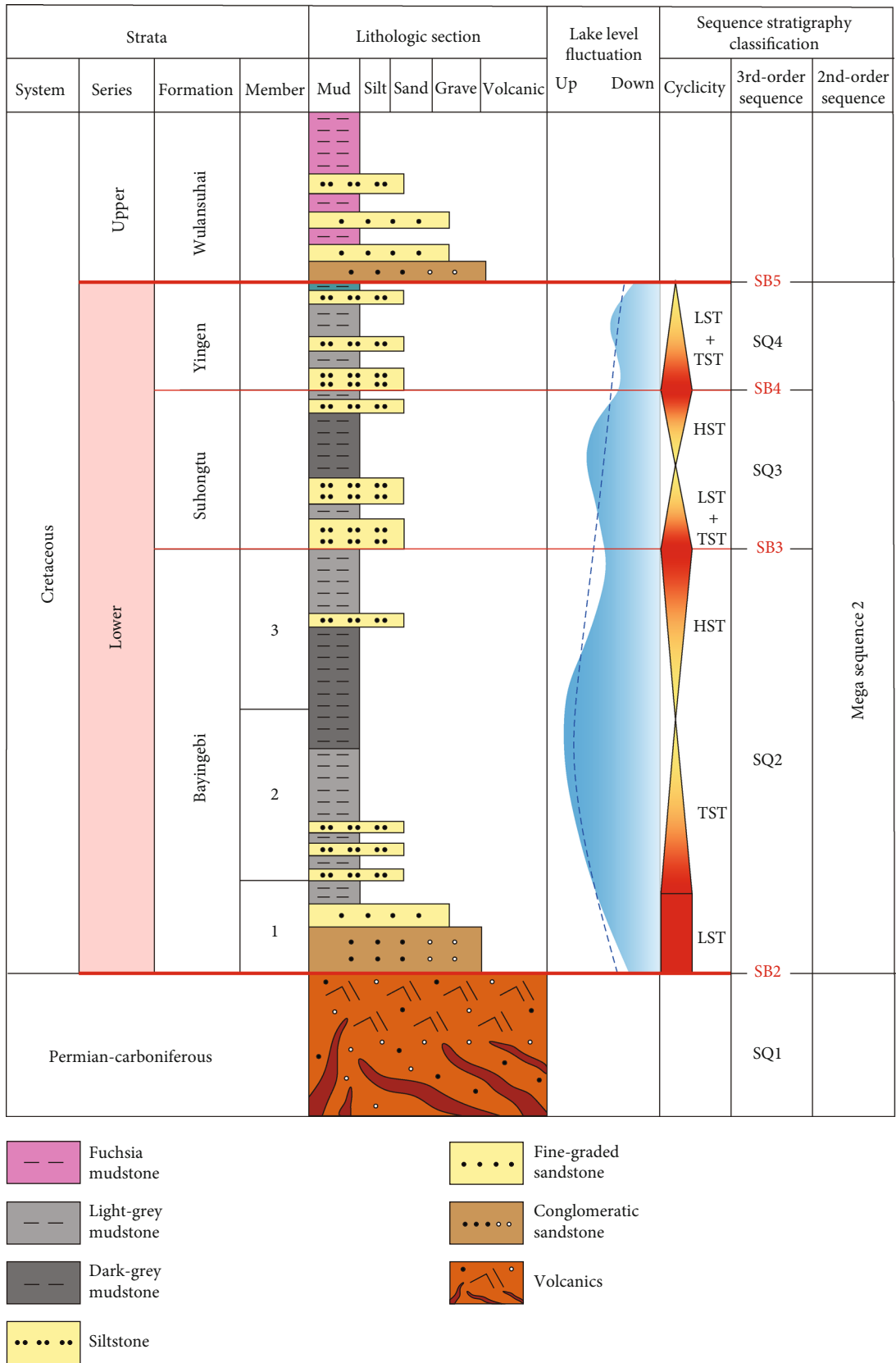
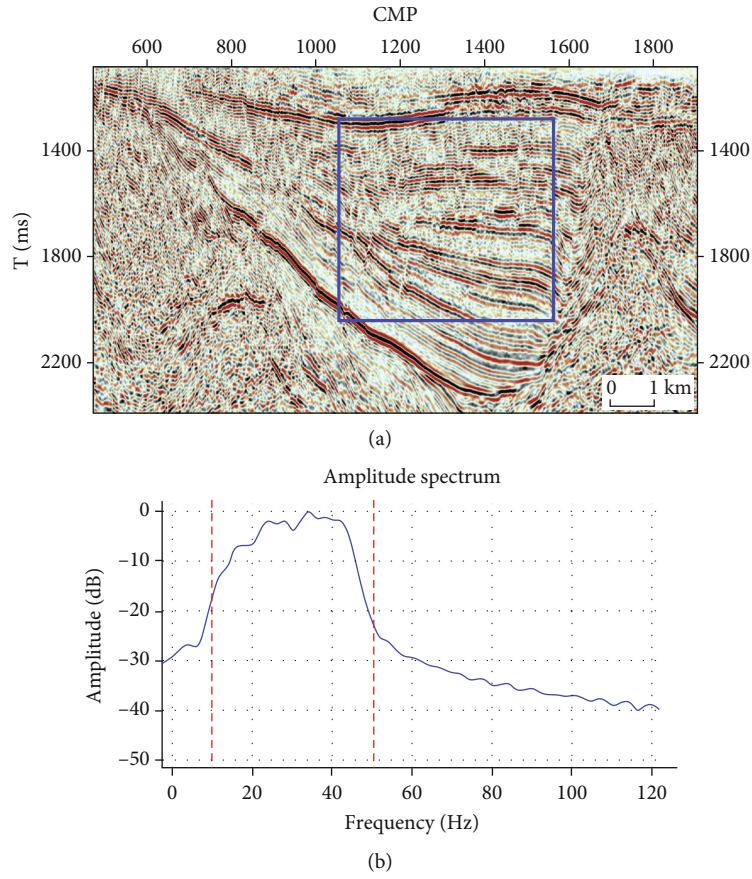FIGURE 2: Lithology and sequence stratigraphic division of the Lower Cretaceous in Aitegle Sag.

(a)

Amplitude spectrum

(b)

FIGURE 3: (a) Seismic reflections and (b) seismic spectra of the Lower Cretaceous interval in Aitegle Sag.
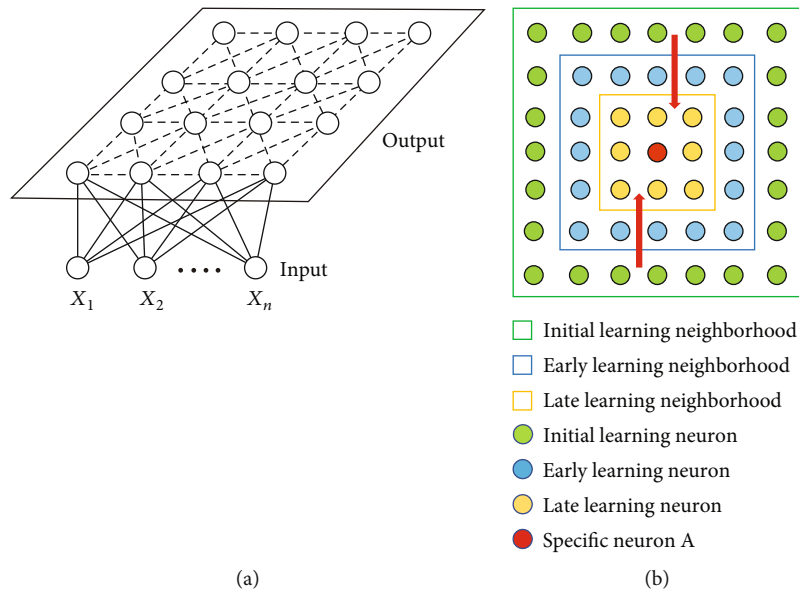

(a)

(b)

FIGURE 4: (a) Self-organizing mapping model and (b) schematic diagram of training range adjustment.

convergence in the learning course is guaranteed.

$$\begin{cases} \Delta W_y = \delta \left(H_x - W_y \right), & y \in N_A, \\ \Delta W_y = 0, & y \notin N_A. \end{cases} \tag{2}$$

The SOM algorithm can be summarized as a process of searching the best matching neuron (the winning neuron) and self-organizing of weights in the network. The best matching neuron represents the best matching of input signal H_x and connection weight W_{xy}. It is represented by Euclidean distance Lo, and the minimum Euclidean distance determines the best matching neuron, i.e., the winning node A.

$$\text{Lo} = \sum_{x=1}^{n} \left(H_x - W_{xy} \right)^2. \tag{3}$$

Early seismic facies classification relies on macroscopic seismic reflection characteristics, so it is a subjective technique. Later, seismic attributes (e.g., amplitude, frequency, and reflection configuration) were introduced into seismic facies analysis. With more and more types and branches of seismic attributes, it is important to use multiple seismic attributes to improve the reliability of seismic facies analysis [40–44].

In seismic facies analysis, it is usually necessary to introduce various seismic attributes related to seismic facies prediction. The introduction of seismic attributes usually goes through a process from less to more and from more to less. Therefore, for specific problems, it is necessary to select the best seismic attribute subset from all seismic attribute sets. This is the seismic attribute optimization problem we need to solve first. In this study, we first selected 10 attributes that are sensitive to the change of seismic facies based on the seismic facies indicators of the profile and carried out correlation analysis on them and selected 4 of them as the input data for seismic attribute cluster analysis. Then, combined with the actual geological characteristics of the scarce wells in the study area, the unsupervised self-organizing mapping network learning algorithm without using training samples is introduced for seismic attribute pattern recognition. Its core is to obtain the SOM density map through neural network learning and further divide the SOM density map. The outstanding feature of this technology is that it can be analyzed interactively; that is, it can combine the researchers' understanding of the work area with computer analysis and effectively realize the seismic facies classification with geological awareness without or with few wells.

4. Sequence Stratigraphy of the Lower Cretaceous

4.1. Identification of Sequence Boundary.
Two second-order sequence boundaries, i.e., SB2 (bottom of the Bayingobi Formation) and SB5 (top of the Yingen Formation), and two third-order sequence boundaries, i.e., SB3 (bottom of the Suhongtu Formation) and SB4 (bottom of the Yingen

Formation), are identified in the Lower Cretaceous (Figure 5).

4.1.1. Second-Order Sequence Boundaries. SB2 showing an abrupt change on the GR log is a large regional unconformity between the Bayingobi Formation and the Carboniferous-Permian. Above SB2 is a thick interval of mottled conglomerate with sandstone, and the conglomerate is almost volcanic rock. Below it is ash black mudstone. On the seismic profile, distinct onlap and truncation are identified near the gentle slope at the margin of the lake basin. Significantly different reflections are observed locally above and below SB2. Specifically, there are sheet, strong-amplitude, continuous parallel reflections above SB2 and chaotic reflections below it.

SB5 is a large regional unconformity between the Yingen Formation and the overlying Wulansuhai Formation. Above it, a thin interval of pebbly sandstone is developed. Below it, purple mudstone with sandstone of the Yingen Formation is deposited. SB5 shows a significant difference in the baseline on the GR log. On the seismic profile, distinct truncation and different seismic reflections are identified above and below SB5. Specifically, chaotic reflections are above it and medium-strong amplitude, continuous, parallel reflections below it, which suggests favorable stratification.

4.1.2. Third-Order Sequence Boundaries. SB3 is an angular unconformity between the Suhongtu Formation and the Bayingobi Formation. The formation occurrence differs greatly above and below it. It is generally dominated by fine clastic deposits. Purer mudstone with less sandstone is developed below it, showing box-shaped log with a high-value baseline. Thin sand-mud interbeds are deposited predominantly above it, presenting finger-shaped log with a low-value baseline. On the seismic profile, distinct truncation and locally different seismic reflections are identified above and below SB3. Specifically, above it are medium-strong amplitude, discontinuous, parallel reflections, and below it are continuous, parallel reflections with strong amplitude.

SB4 is an angular unconformity between the Yingen Formation and the Suhongtu Formation. Above it is purer mudstone with less sandstone, showing box-shaped log with a high-value baseline. Thin sand-mud interbeds are deposited predominantly below it, presenting finger-shaped log with a low-value baseline. Distinct onlap reflections are identified at the margin of the lake basin, and the bottom of the Yingen Formation characterized by strong-amplitude and continuous seismic reflections is traceable laterally.

4.2. Sequence Correlation and Sequence Stratigraphic Framework. The Lower Cretaceous is divided into one second-order sequence, three third-order sequences (SQ2–SQ4), and six system tracts. Based on the sequence classification of the adjacent Hari Sag, the sequence classification of the Lower Cretaceous in the study area starts with SQ2 to keep in line with the existing sequence names. SQ2 has a complete trichotomy structure, SQ3 has a dichotomy
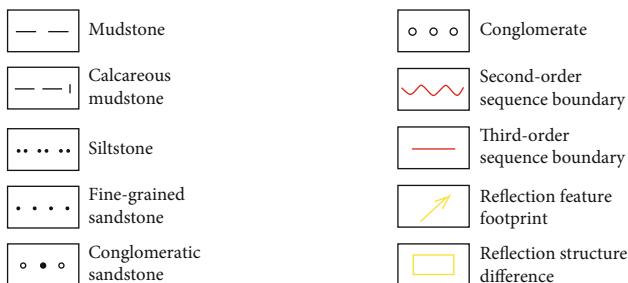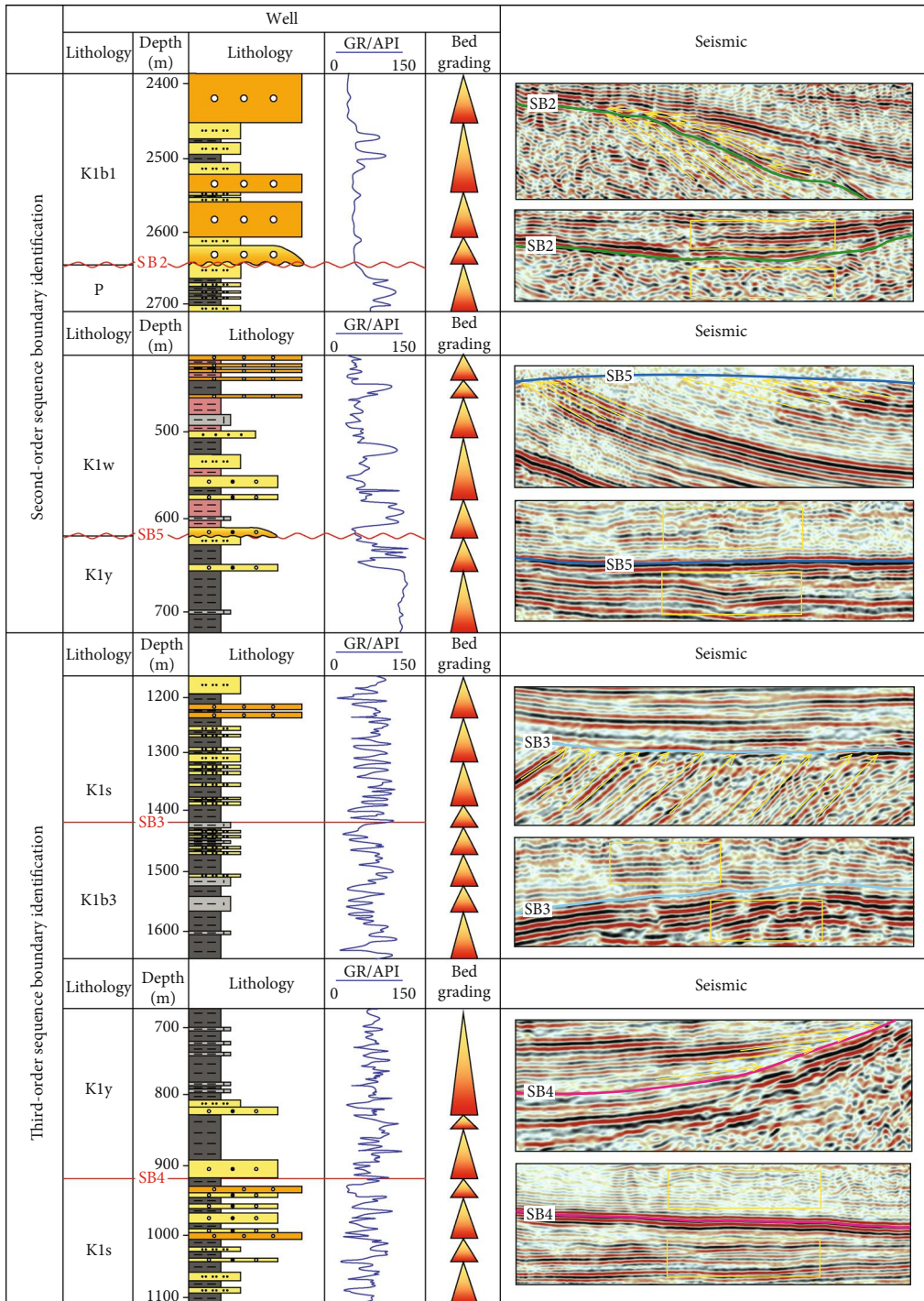
FIGURE 5: Well seismic response characteristics of sequence stratigraphic boundaries of the Lower Cretaceous.
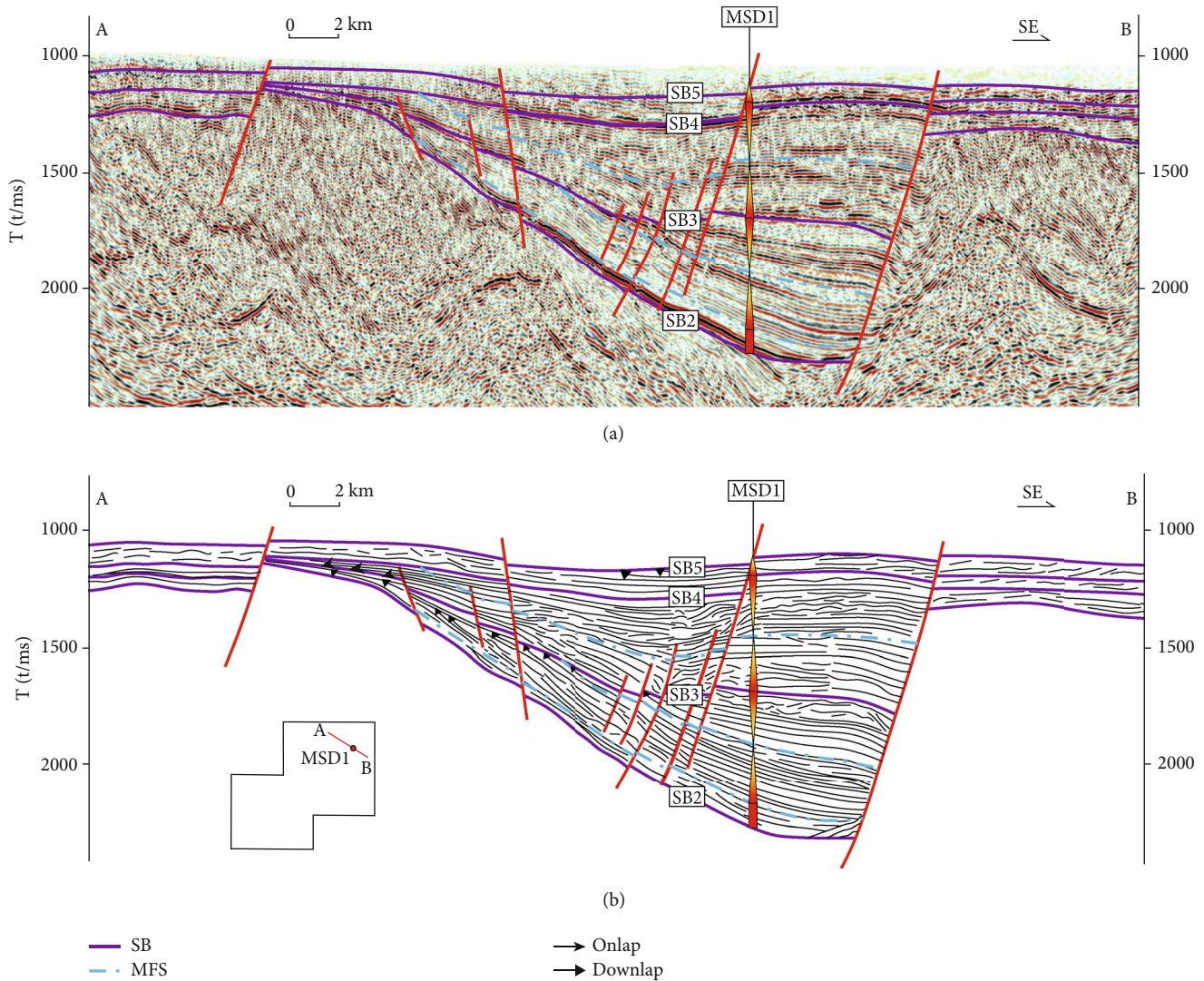
(a)

(b)

FIGURE 6: (a) Seismic profile through well MSD1 and (b) sequence stratigraphic framework based on well seismic data (MSD1).

structure, and SQ4 has an incomplete structure since the highstand system tract (HST) was denuded.

On the basis of the sequence stratigraphic classification for well MSD1, the sequence stratigraphic framework was established, which is vertical to the structural trend along the through-well seismic profile (Figure 6).

As shown on the seismic profile, the fault lake basin has a structure with morphological integrity, and the Lower Cretaceous, which was penetrated by well MSD1, has downlap and toplap reflection patterns near SB3 in the gentle slope at the margin of the lake basin. In the deep depression zones next to the deep and large faults, the three third-order sequences included in the Lower Cretaceous strata are easy to be distinguished and identified due to their greatly different reflection patterns.

SQ2 is remarkably trichotomous in its internal structure. The formation dip changes significantly at the bottom of the deep and large fault in the lowstand system tract (LST), the seismic reflections of the lacustrine transgressive system tract (TST) are more continuous and layered, and those of

the highstand system tract (HST) show slightly poor continuity. SQ3 is dichotomous. In the deep depression zones, the TST shows stronger amplitude reflections with better continuity, and the HST shows weaker amplitude reflections with slightly poorer continuity. SQ4 has an incomplete structure with missing HST. Its seismic reflections are poorly layered and significantly different from those of SQ2 and SQ3.

5. Types and Characteristics of Sedimentary Facies in Sequence Stratigraphic Framework

5.1. Sedimentary Facies Marks. Delta, lake and sublake fan are the major types of sedimentary facies identified in the Lower Cretaceous. According to the tectonic-geological characteristics, lithological associations and seismic facies, delta plain-front, prodelta-shore-shallow lake, semideep lake, deep lake, and sublake fan subfacies are further identified.
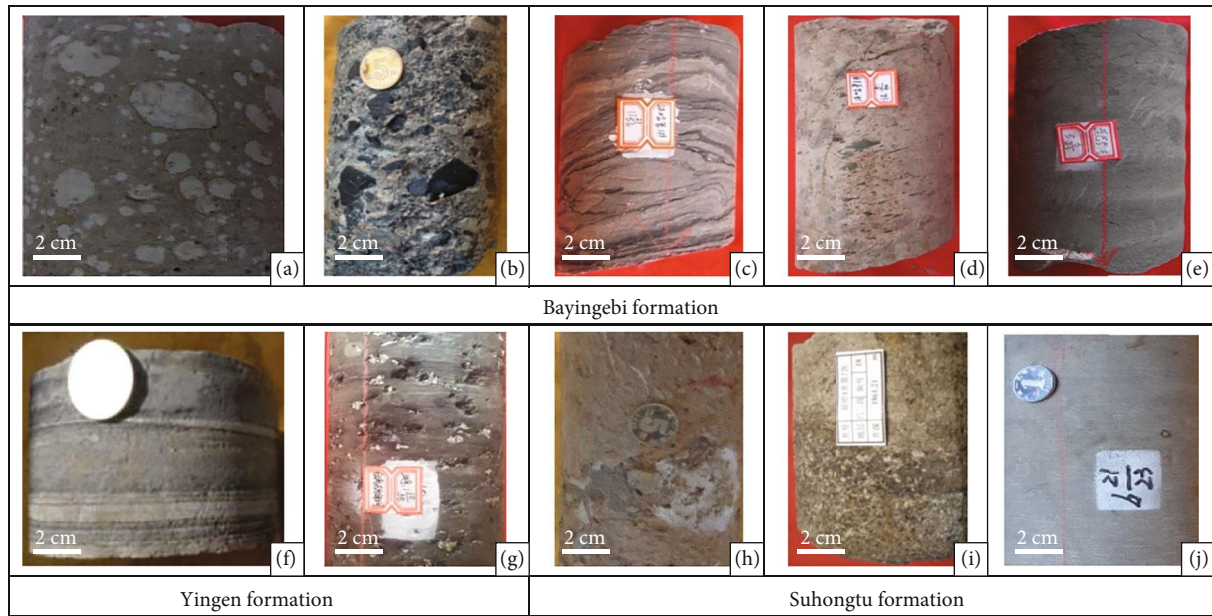
FIGURE 7: Typical cores from the Lower Cretaceous in Hari Sag. (a) Basalt gravel, Bayingobi Formation, well YH3. (b) Mottled glutenite, Bayingobi Formation, well YH2. (c) Convolute bedding, Bayingobi Formation, well YHC1. (d) Dacite, Bayingobi Formation, well YHC1. (e) Massive bedding, Yingen Formation, well YBC1. (f) Parallel bedding, Yingen Formation, well YH4. (g) Dolomitic mudstone, Yingen Formation, well YHC1. (h) Massive mud pebble, Suhongtu Formation, well YBN1. (i) Graded bedding, Suhongtu Formation, well YH4. (j) Massive bedding, Suhongtu Formation, well YHC1.
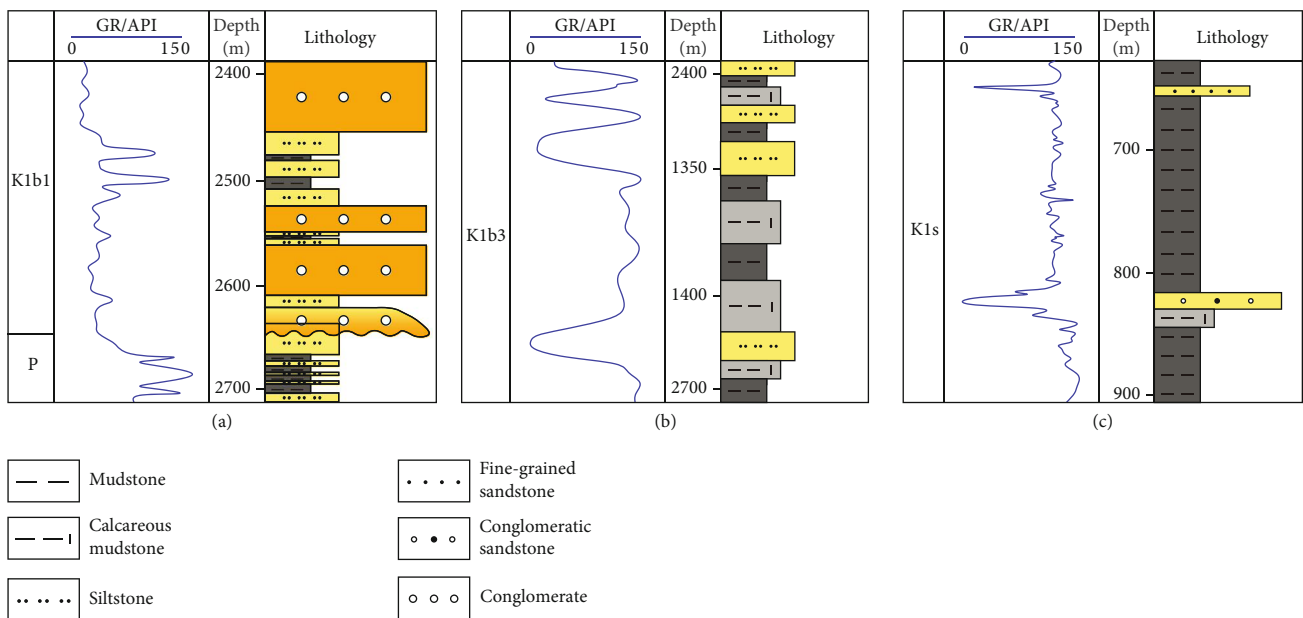

FIGURE 8: Typical logging facies in wells MSD1 and AI2, Aitegle Sag. (a) Turbidite sand in a box-shaped structure with low GR values; (b) shore-shallow lake deposits with alternating medium-high GR and low GR thin beds; (c) deep lake mudstone with medium-high GR values.

5.1.1. Lithofacies. Without core data of the Aitegle Sag, abundant core data of the Hari Sag that has similar seismic and geological characteristics to the Aitegle Sag are used for sedimentary facies analysis (Figure 7).

SQ2 (the Bayingobi Formation) is mainly composed of medium-coarse sandstone and conglomerate which are poorly sortable and medium-poorly round and have parallel, massive, and convolute beddings that indicate high hydrodynamic deposits.

SQ3 (the Suhongtu Formation) mainly consists of siltstone and fine sandstone with graded and massive beddings.

SQ4 (the Yingen Formation) is mainly composed of siltstone and dolomitic mudstone with plant debris, biological remains, and parallel bedding.
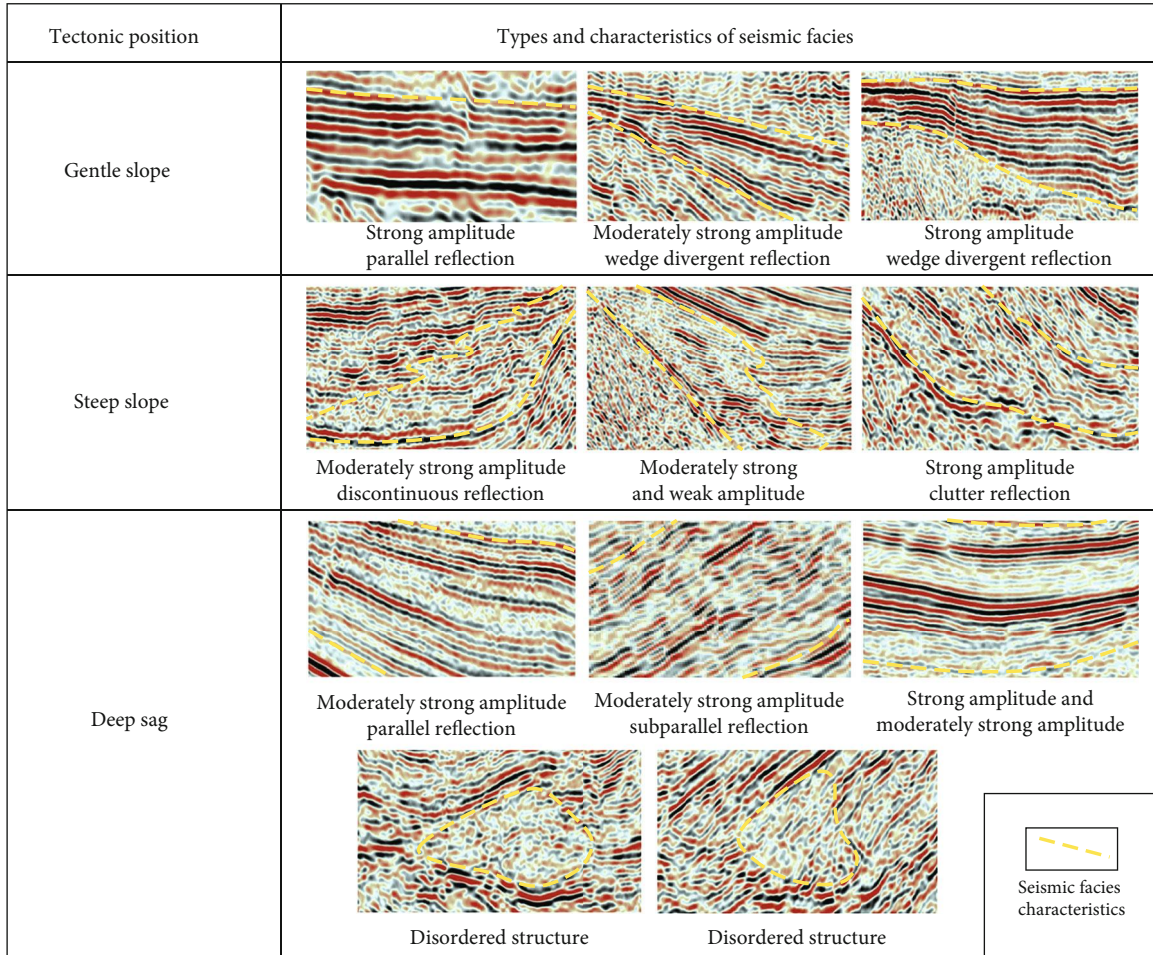
Tectonic position	Types and characteristics of seismic facies		
Gentle slope	Strong amplitude parallel reflection	Moderately strong amplitude wedge divergent reflection	Strong amplitude wedge divergent reflection
Steep slope	Moderately strong amplitude discontinuous reflection	Moderately strong and weak amplitude	Strong amplitude clutter reflection
Deep sag	Moderately strong amplitude parallel reflection	Moderately strong amplitude subparallel reflection	Strong amplitude and moderately strong amplitude
	Disordered structure	Disordered structure	Seismic facies characteristics

FIGURE 9: Typical seismic facies of different structural zones in Aitegle Sag.

Attribute	LyapIndex	FrctDim	InfoEntr	RMSAmp	IntAbsAmp	I Band	I Freq	I Phase	IReAmp	25% Freq
LyapIndex	1.0000									
FrctDim	0.3259	1.0000								
InfoEntr	0.2628	0.7594	1.0000							
RMSAmp	0.2862	0.1528	0.2505	1.0000						
IntAbsAmp	0.2471	0.7497	0.9842	0.1508	1.0000					
I Band	0.0544	0.0367	0.0030	0.1062	0.0078	1.0000				
I Freq	0.1592	0.0912	0.0410	0.0910	0.0493	0.0439	1.0000			
I Phase	0.0088	0.0873	0.0913	0.0979	0.0745	0.0256	0.0314	1.0000		
IReAmp	0.0429	0.0436	0.0313	0.0153	0.0046	0.0477	0.0168	0.0001	1.0000	
25% Freq	0.1494	0.2692	0.3320	0.1922	0.3324	0.0002	0.0037	0.0104	0.0037	1.0000

FIGURE 10: Correlation coefficient matrix of seismic attributes.

5.1.2. Logging Facies. Based on GR log and logging-derived lithology data, the logging facies were analyzed (Figure 8). The typical logging facies exhibit sublake fan turbidite sands in a nearly box-shaped structure with low GR values, shore-shallow lake deposits with alternating medium-high GR and low GR thin beds, and semideep-deep lake mudstone with medium-high GR values.

5.1.3. Seismic Facies. After a comparative analysis of seismic data, 10 seismic facies marks were identified. They are (a) in the gentle slope zone, the seismic facies with medium-strong amplitude, parallel-subparallel reflections at structural highs, and the seismic facies with medium-strong amplitude, wedge-shaped, divergent reflections in the basinward part; (b) in the steep slope zone, the seismic facies with
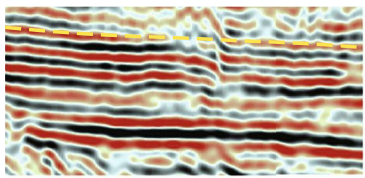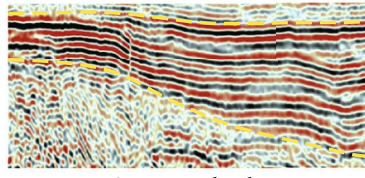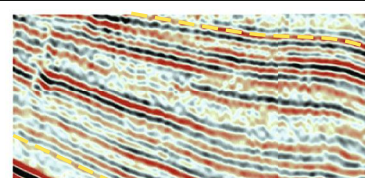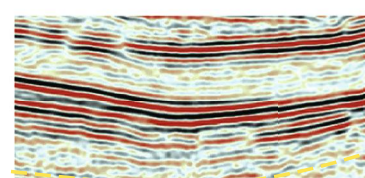
Type	Characteristics of seismic section	Location	Sedimentary facies
1	Strong amplitude parallel reflection	Gentle slope (towards the shore)	Delta plain
2	Strong amplitude wedge divergent reflection	Gentle slope (towards the center of the lake)	Delta front
3	Moderately strong amplitude parallel reflection	Steep slope	Shore shallow lake
4	Strong amplitude and moderately strong amplitude	Deep sag	Semi deep lake - deep lake

FIGURE 11: Types of seismic facies in the Lower Cretaceous strata.

discontinuous, divergent, hummocky reflections with medium-strong amplitude, the discontinuous reflections in the part extending towards the lake basin along the synsedimentary deep and large faults, and the seismic facies with medium-strong amplitude, wedge-shaped, divergent reflections in the part extending towards the lake basin along the faults with small dips; and (c) in the deep depression zone, the seismic facies with medium-strong amplitude, continuous-relatively continuous, parallel-subparallel reflections, the seismic facies with high amplitude, continuous sheet reflections, the seismic facies with weak amplitude, nearly blank seismic reflections, and the seismic facies with weak amplitude, mound-shaped chaotic reflections near the bottom of the deep and large faults (Figure 9).

5.2. Classification of Seismic Facies by Seismic Attribute Clustering Based on SOM Algorithm

5.2.1. Extraction and Selection of Seismic Attributes. Targeting at system tracts, 53 kinds of seismic attributes, including instantaneous, amplitude, and spectral attributes, were extracted. Based on the seismic facies marks, 10 kinds of attributes sensitive to the change of seismic facies were selected, and their correlation coefficients were collected. A correlation coefficient greater than 0.8 indicates one redundant attribute in two attributes, which will be deleted. A correlation coefficient less than 0.2 indicates no correlation between two attributes, which are not appropriate for clustering.

Statistical results reveal that four seismic attributes, i.e., LyapIndex, FrctDim, InfoEntr, and RMSAmp, have correlation coefficients ranging from 0.25 to 0.75, which are used as the basis for clustering (Figure 10).

5.2.2. Seismic Attribute Clustering Based on SOM Algorithm. Identification of sectional seismic facies was carried out for determining suitable classification parameters. As described in Section 5.1.3, 9 seismic facies marks were effectively identified at different structural positions. For the purpose of satisfactory classification and simplified calculation, 4 representative and distinguishable seismic facies marks at different structural positions were selected as the references for classification. These seismic facies marks include (1) the seismic facies with strong amplitude, parallel-subparallel
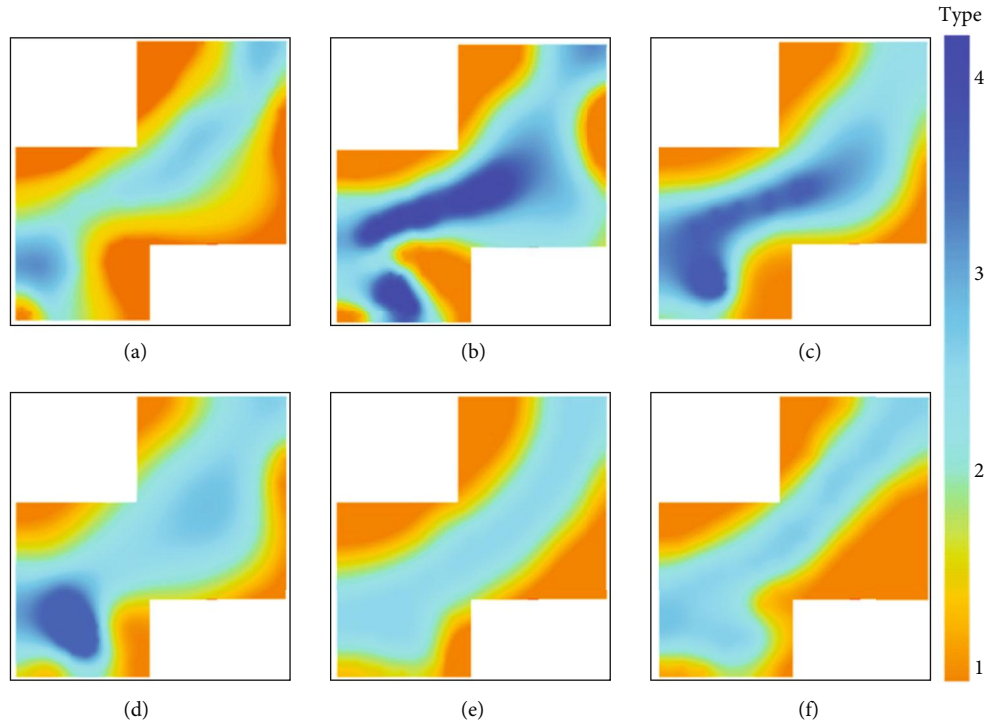
FIGURE 12: SOMA-based seismic attribute clustering results of the Lower Cretaceous strata in Aitegle Sag. (a) SQ2-LST, (b) SQ2-TST, (c) SQ2-HST, (d) SQ3-LST+TST, (e) SQ3-HST, and (f) SQ4-LST+TST

reflections in the gentle and steep slope zones; (2) the seismic facies with medium-strong amplitude, wedge-shaped, divergent reflections in the gentle slope zone; (3) the seismic facies with discontinuous, divergent reflections in the steep slope; and (4) the seismic facies with medium-strong amplitude, continuous-relatively continuous, parallel-subparallel reflections in the deep depression zone (Figure 11).

After clustering of these seismic attributes, the study area is divided into four zones, i.e., zone 1 in orange, zone 2 in yellow-green, zone 3 in blue, and zone 4 in dark blue. Certain relations exist between the clustering results of system tracts. Zone 1 is distributed in the northwestern and southeastern parts of the study area, and zone 3 is distributed in the central part of the study area. Some differences are also found between the clustering results of system tracts. According to the clustering results of seismic attributes for LST of SQ2, in the northeastern and locally western part of the study area, zone 2 extends extensively towards the lake basin center, which is greatly different from the clustering results of other system tracts. Zone 4 varies greatly in the system tracts (Figure 12).

6. Sequence-Sediment Filling Evolution

6.1. Responses of Sequence and Sediment Fillings

6.1.1. SQ2. SQ2 corresponding to the initial rifting stage is a complete trichotomous sequence. Its LST mainly composed of sublake fan turbidite sand bodies is located in the deep depression zone at the bottom of large faults and only dis-

tributed in the northeastern and western parts of the study area. As the faults extended to deeper formations and the accommodation space increased, the LST transformed into a TST, and the deposits of lacustrine facies began to develop extensively. At the end of the second member of the Bayingobi Formation, the lake rose to a high level and also to the highest within the whole second-order sequence. With the slowing down of faulting, sediment supply from NW and SE increased, and the TST transformed into a HST. During the deposition of the third member of the Bayingobi Formation, the lake level gradually dropped, and the delta-shore-shallow lake facies expanded (Figures 13 and 14).

6.1.2. SQ3. SQ3, corresponding to the faulted depression-sag transition stage, is a dichotomous sequence. As tectonic movement intensified and faulting enhanced, the accommodation space increased, and the HST of SQ2 transformed into the TST of SQ3. The deposits of lacustrine facies were developed extensively and the lake basin expanded. The lake level rose to the highest in the middle period of the Suhongtu Formation. As faulting slowed down, the sediment supply from NW and SE increased, and the TST transformed into the HST. At the end of the Suhongtu Formation, the lake level gradually fell, and the delta-shore-shallow lake facies gradually expanded (Figures 13 and 14).

6.1.3. SQ4. SQ4, corresponding to the end of depression, is an incomplete sequence where there only remain LST and TST, but the HST is missing. During the early stage of SQ4, faulting activities continued, the accommodation space gradually reduced, and the HST of SQ3 transformed into the
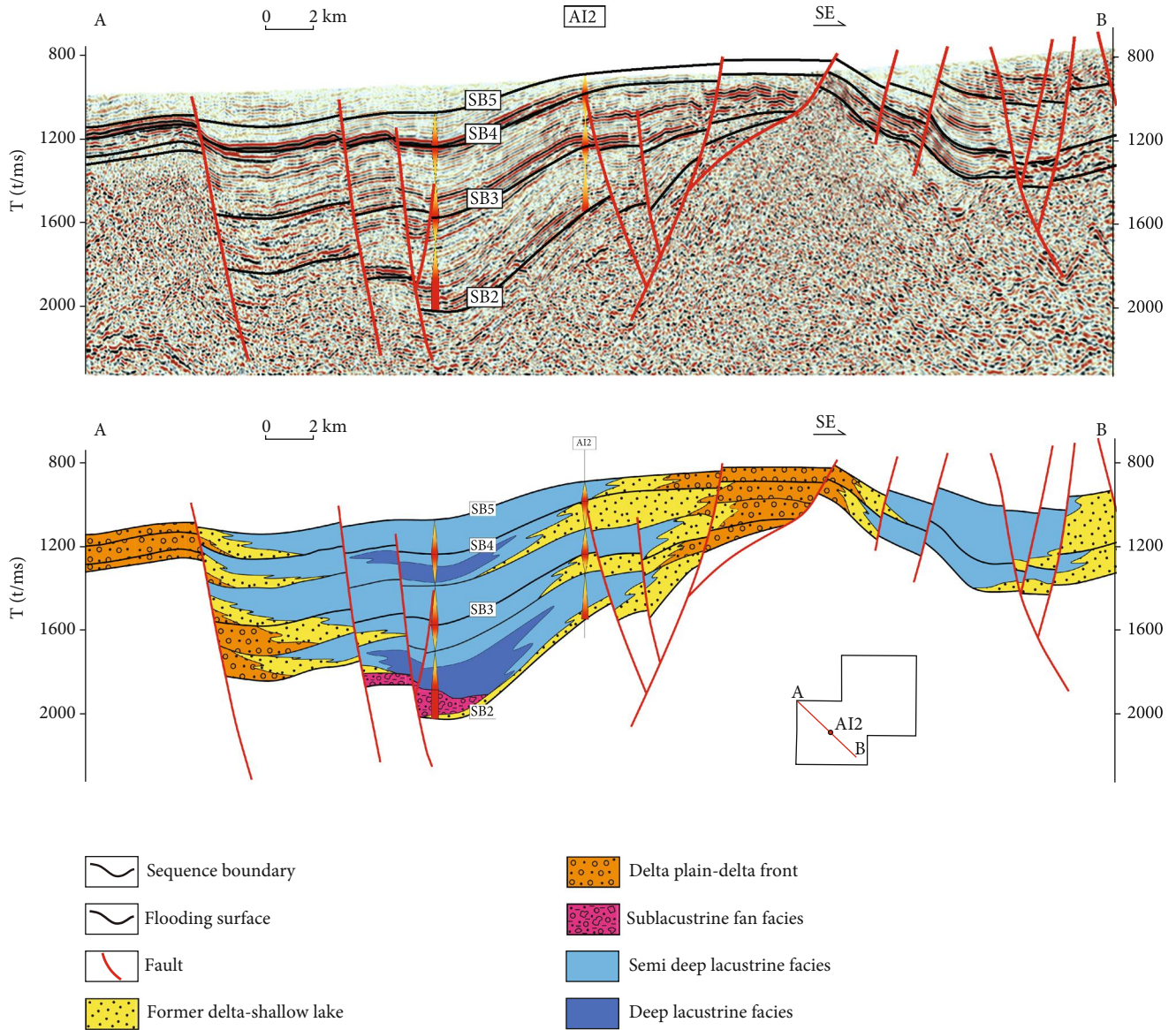
FIGURE 13: Sequence-sediment filling responses of the southern subsag in Aitegle Sag.

TST of SQ4. The deposits of lacustrine facies were developed. In the early period of the Yingen Formation, the lake level rose to the highest, and the whole area was almost covered by the deposits of shore-shallow lake facies. Comparative analysis indicates that SQ4 has a significantly smaller residual thickness than SQ2 and SQ3. It is concluded that the HST of SQ4 has been denuded (Figures 13 and 14).

6.2. Plane Evolution Processes of Sedimentary System. All system tracts in the Lower Cretaceous are dominated by the deposits of delta-shore-shallow lake subfacies and semideep-deep lake subfacies, and they also contain sublake fan facies of the LST of SQ2. The sources were mainly from two directions: NW and SE. The delta formed by the deposits sourced from the northwest shows stable progradation in all system tracts, and that from the southeast varies greatly in different system tracts (Figure 15).

6.2.1. SQ2. In the LST period, the delta-shore-shallow lake system was developed extensively in the northwestern and southeastern parts of the study area. The sublake fan facies was deposited at the lake entrance in the front of the delta-shore-shallow lake system and in an area parallel to the shoreline. The lake basin subsided to the deepest at the southwest corner of the study area. In the TST period, along with intensified tectonic movements, the accommodation space increased, and the extensive delta-shore-shallow lake system in the northwestern and southeastern parts was gradually replaced by the deposits of lacustrine facies. As the lake level rose, the lake basin expanded to the largest in the whole period of the second-order sequence, and deep-water areas were formed widely and dominantly located in the central and western parts of the study area. In the HST period, the delta-shore-shallow lake system began to prograde towards the lake basin and generally entered it in oblique
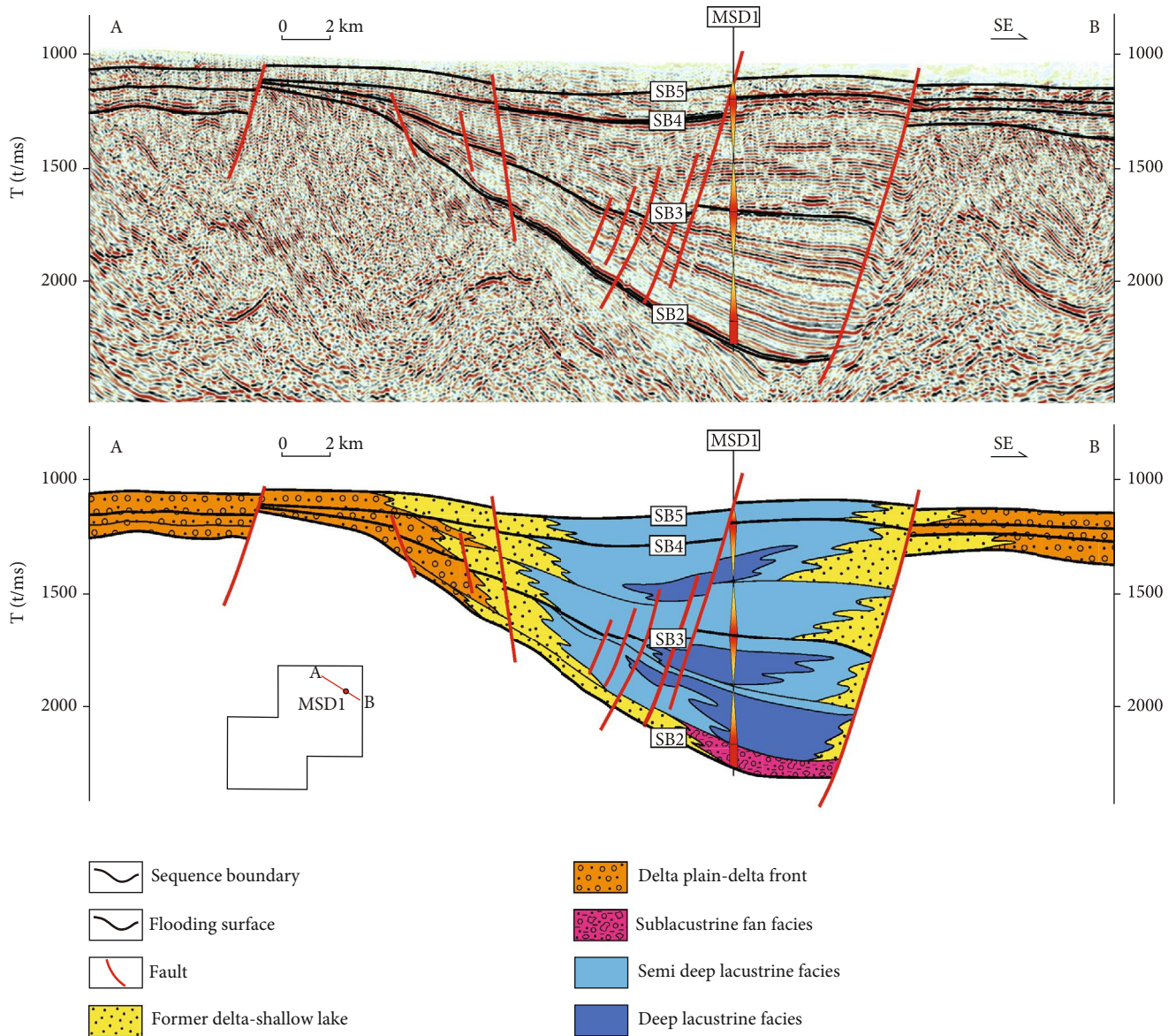
FIGURE 14: Sequence-sediment filling responses of the northern subsag in Aitegle Sag.

arrangement, showing distinct progradational configuration on the seismic profile. As the lake level dropped, the deepest part of the lake basin started to migrate from the central part to the western part.

6.2.2. SQ3. In the TST period, the accommodation space increased, and the extensive delta-shore-shallow lake system in the northwestern and southeastern parts was gradually replaced by the deposits of lacustrine facies. As the lake level rose, the lake basin expanded, with the deepest parts mainly located in the southwestern part. However, the water was obviously shallower than that in the SQ2 period. In the HST period, the delta-shore-shallow lake system began to prograde towards the lake basin with the falling of lake level. The delta formed by the sediments from SE advanced towards the lake basin center significantly, and the water depth decreased.

6.2.3. SQ4. In the SQ4 period, i.e., at the end of depression, the deposits of delta-shore-shallow lake facies were developed extensively and were close to the surface as shown on the seismic profile. The shape of the lake basin remained only at the deep depression zone. SQ4 was deposited stably and distinctly thinner than SQ2 and SQ3. Based on seismic and well data, SQ4 is deemed to only have deposits of LST and TST. The deposits of delta-shore-shallow lake facies inherited the scope of those in SO3, but the HST was denuded.

7. Discussion

7.1. Controlling Factors for Sequences. At present, it is recognized by the method of palynology that the climate environment of Yin'e Basin changed from dry and hot to warm and humid during the Lower Cretaceous sedimentary period [45,

(a)

(b)

(c)

(d)

↑N   0   20 km

(e)

(f)

Former delta-shallow lake

Delta plain-delta front

Sublacustrine fan facies

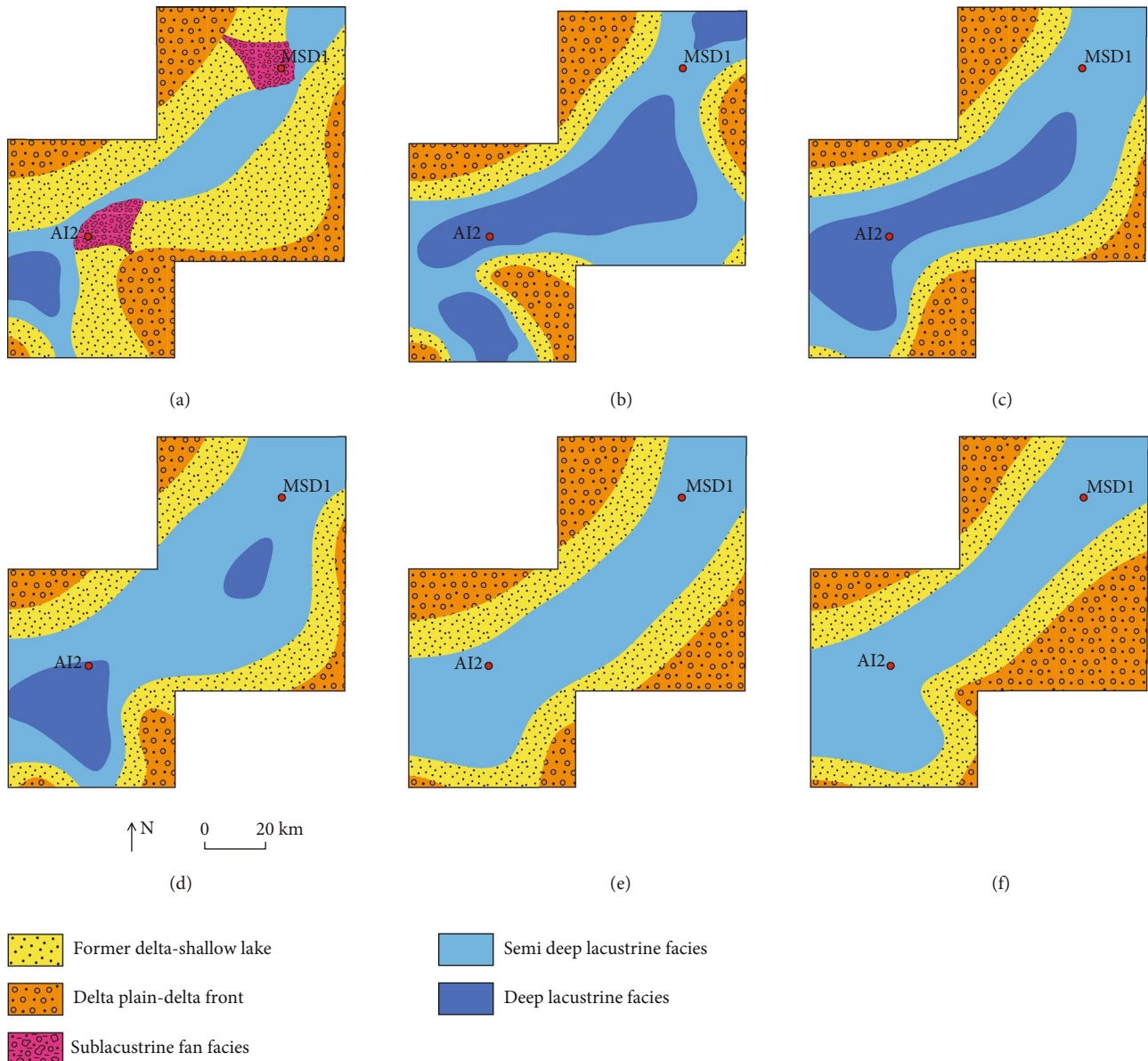Semi deep lacustrine facies

Deep lacustrine facies

FIGURE 15: Planar evolution of sequence-sedimentary system in Aitegle Sag: (a) SQ2-LST, (b) SQ2-TST, (c) SQ2-HST, (d) SQ3-LST+TST, (e) SQ3-HST, and (f) SQ4-LST+TST.

46]. Under the background of large climate change, the sequence development characteristics are further affected by the comprehensive effects of structure, lake level, and material supply [47–50].

In the LST period, at the beginning when the lake basin was rifted, the basin formed by tectonic movements was characterized by small accommodation space, a large amount of sediments from the uplifts on the sides, and a small lake area (Figure 15(a)). The basin was dominated by delta deposits. At the end of prodelta, local deposits, which were obviously different with those in its peripheral areas, were generally developed at the bottom of deep and large faults and show distinct chaotic seismic reflections (Figure 9, disordered structure). It is revealed by well data that thick mixed deposits were developed, including fine and coarse grains (Figure 8(a)).

In the TST period, with the rifting of the lake basin, the accommodation space was expanded by tectonic movements, presenting as the greatly expanded lake area and increased water depth. The sedimentary facies in the transition zone from the small uplift in the southeastern part of the study area to the Maima Sag transformed distinctly from LST prodelta deposits into TST lake deposits (Figures 15(b) and 15(d)). As the sediments originated from the uplifts on the sides reduced, the distribution of delta facies decreased significantly.

The comparison of LST and TST sedimentary models shows that tectonic movement is the main controlling factor for the development of Lower Cretaceous sequence in Aitegle Depression. The change of lake water level is mainly affected by the comprehensive influence of climate factors and tectonic movement, especially by the control
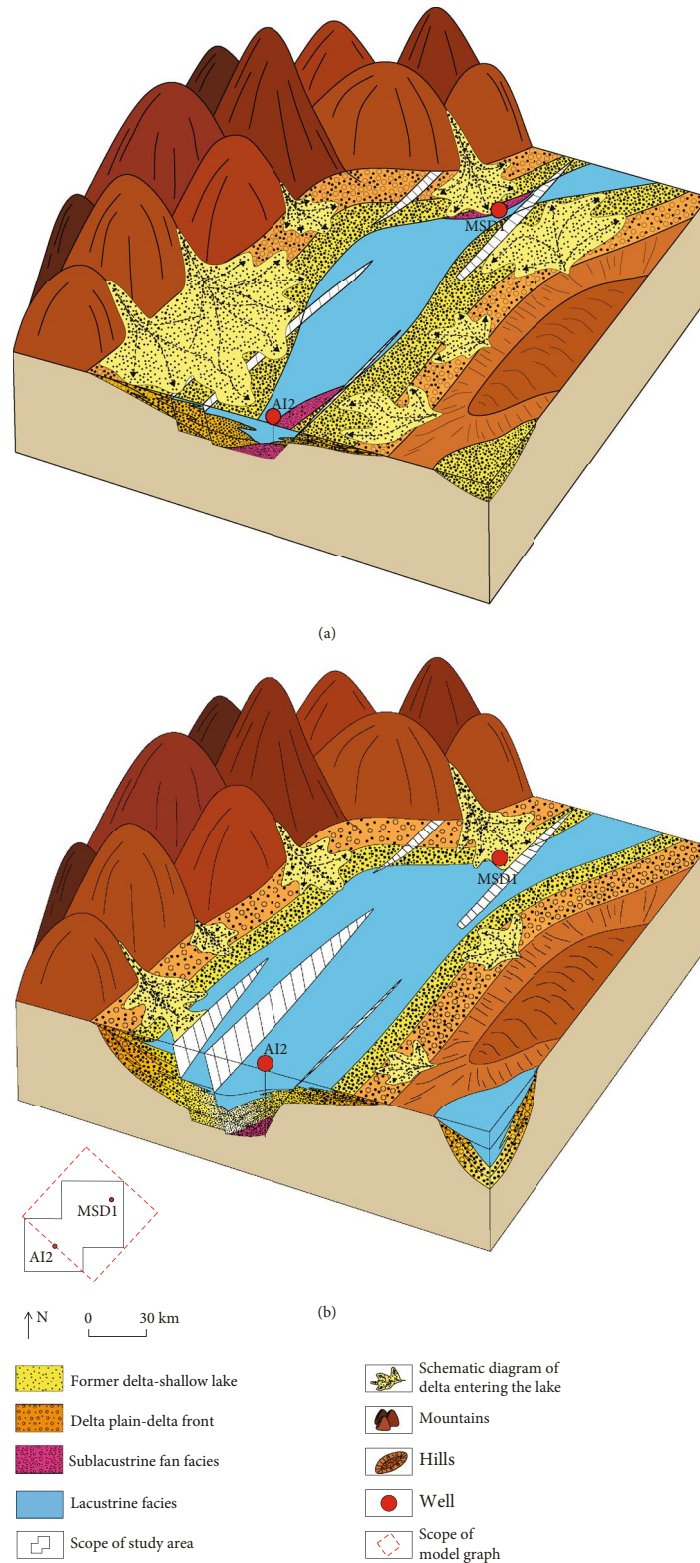
(a)

(b)

FIGURE 16: Correlation of sequence-sedimentary models in Aitegle Sag. (a) LST and (b) TST.

faults of large depressions (Figure 16). The combination of lake water level changes and sediment supply from two directions affected the development of sedimentary facies belts in different system tracts within the third-order sequence.

In future oil and gas exploration and development, research focuses should be on the phases of tectonic movement, fault characteristics, and sediment supply changes resulted from the Aogao uplift and small uplifts in the southeastern part of the study area (Figure 1(e)).

7.2. Application and Significance of Seismic Attribute Clustering Based on SOM Algorithm. A new idea for sequence-sediment research is proposed for new exploration areas with scarce wells. In the case of only 2D seismic data and limited logging data available, the SOM clustering technique is introduced to seismic attribute clustering in line with geologic characteristics. Thus, a bridge is established between seismic facies and sedimentary facies. Generally, the research results are considered significant in two aspects.

(1) The integration of SOM with seismic attribute clustering allows an effective combination of geophysical methods based on big data with geological analysis (Figure 12), which is significant for guiding the sequence-sediment research on the fault basin regions with scarce wells. The SOM algorithm is essentially a self-organizing learning process without samples, and it is consistent with the situation of exploration areas with scarce wells. Their integration strengthens the utilization of seismic data and guarantees the validity and reliability of the clustering results

(2) The technique of seismic attribute clustering based on SOM algorithm can basically illustrate the distribution laws of sedimentary facies in system tracts (Figure 15) and support further exploration in new areas with scarce wells. It is very suitable for the areas with high-quality seismic data (e.g., the Aitegle Sag) which clearly reflect identifiable seismic reflections and abundant geological phenomena. In the process of regional survey, more effective geological information in addition to structural characteristics can be obtained to support subsequent exploration and development with lower cost and higher benefits. Of course, along with the innovation of seismic techniques, a breakthrough will be made to the dominant frequency, bandwidth, and resolution of seismic data, which means higher precision of sequence-sediment research based on seismic data

8. Conclusions

(1) Sequence classification and sequence stratigraphic framework have been established for the Lower Cretaceous in the Aitegle Sag. The Lower Cretaceous is divided into one second-order sequence, three third-order sequences (SQ2–SQ4), and six system tracts. SQ2 is a trichotomous sequence, SQ3 is a dichotomous sequence, and SQ4 is lack of HST in the study area

(2) Five sedimentary subfacies, i.e., delta plain-front, prodelta-shore-shallow lake, semideep lake, deep lake, and sublake fan, were identified in the Lower Cretaceous. The deposits of delta-shore-shallow lake subfacies in the gentle slope zone mainly show medium-strong amplitude, wedge-shaped, divergent seismic reflections, and those in the steep slope zone mainly show discontinuous, divergent, hummocky

seismic reflections. The deposits of semideep-deep lake subfacies in the deep depression zone mainly present medium-strong amplitude, continuous-relatively continuous, parallel-subparallel seismic reflections. The deposits of sublake fan subfacies present weak amplitude, mound chaotic seismic reflections near the bottom of deep and large faults

(3) The sedimentary evolution laws of the Lower Cretaceous in the Aitegle Sag were clarified. Three changes of sea level occurred in the process of sequence evolution. SQ2 has a complete structure with a clear LST. At the end of the TST, the lake basin reached its largest area in the whole second-order sequence, where the sedimentation-subsidence centers were mainly located in the central-northwestern part of the study area. SQ3 has indistinguishable LST and TST. At the end of the HST, the sediments sourced from SE showed different degrees of progradation, the lake shape changed, and the sedimentation-subsidence centers were mainly situated in the southwestern part of the study area. SQ4 is lack of the HST. In the LST and TST periods, the form of delta-shore-shallow lake subfacies inherited that of SQ3, when the lake basin slightly expanded

(4) We innovatively introduces self-organizing mapping neural network analysis technology into the process of seismic geological research, combines unsupervised self-organizing neural network learning algorithm with seismic attribute clustering analysis process, and effectively realizes the combination of geophysical methods based on massive data analysis and geological problem analysis. The result of seismic facies zoning conforms to the regional sedimentary geological law, which can guide the sequence-sedimentary study of new oil and gas exploration areas with few wells in continental fault basins, and indicates the directions for exploration and development of unconventional and conventional oil and gas reservoirs

Data Availability

Due to the need for confidentiality of basic data, some basic data cannot be disclosed. This study focuses on the innovation and application of technical methods.

Conflicts of Interest

The authors declare that they have no conflicts of interest.

Acknowledgments

References

[1] M. B. Wu and X. M. Wang, "Petroleum geological characteristics and prospecting directions for oil and gas in Yingen-Ejinaqi Basin," *China Petrleum Exploration*, vol. 8, no. 4, pp. 45–49, 2003.

[2] Q. L. Chen, P. S. Wei, and Z. L. Yang, "Tectonic evolution and petroleum prospection in the Yin'Gen-Ejina Basin," *Petroleum Geology & Experiment*, vol. 28, no. 4, pp. 311–315, 2006.

[3] C. Y. Liu, C. S. Lin, M. B. Wu, G. Gong, and M. L. Zheng, "Tectonic evolution and petroleum prospects of the Mesozoic Inggen-Ejin qi basin, Inner Mongolia," *Geology in China*, vol. 33, no. 6, pp. 1328–1335, 2006.

[4] J. Liu, X. Luo, H. Li, and X. Li, "Geochemical characteristics of hydrocarbon source rocks of the lower cretaceous in the Chagan sag," *Lithologic Reservoirs*, vol. 25, no. 1, 2013.

[5] G. C. Yang, D. Q. Jiao, B. Xiao, M. Q. Chen, J. J. Liu, and Y. L. Wang, "Tectono-sequence-sedimentary characteristics, basin prototypes and their genetic mechanisms in Chagan sag of Yin-E Basin, Inner Mongolia," *Journal of Palaeogeography*, vol. 15, no. 3, pp. 305–316, 2013.

[6] X. Y. Bai, Y. H. He, L. Y. Ren, F. X. Ma, H. C. Liu, and X. D. Wang, "Tectonics and evolution of the west Suhongtu depression in Yingen-Ejinaqi Basin," *Journal of Yanan University (Natural Science Edition)*, vol. 36, no. 2, pp. 57–61, 2017.

[7] R. Feng, Y. Zuo, M. Yang et al., "Present terrestrial heat flow measurements of the geothermal fields in the Chagan Sag of the Yingen Ejinaqi Basin, Inner Mongolia, China," *Acta Geologica Sinica - English Edition*, vol. 93, no. 2, pp. 283–296, 2019.

[8] G. Li, W. Qi, and T. Fan, "Prospects for oil and gas exploration in Juyanhai depression," *Journal of Oil and Gas Technology*, vol. 29, no. 5, 2007.

[9] C. C. Zhao, H. C. Liu, L. Y. Ren et al., "Geological environment and prospective significance of cretaceous gas reservoir in well YHC1 of Yin'e basin," *Natural Gas Geoscience*, vol. 28, no. 3, pp. 439–451, 2017.

[10] J. Lu, B. Song, Y. Niu, X. Wei, J. Wei, and H. Xu, "The age constraints on natural gas strata and its geological significance of well Y in Hari depression, Yingen-Ejin basin," *Geological Bulletin of China*, vol. 37, no. 1, pp. 93–99, 2018.

[11] J. Lu, J. Wei, T. Jiang, H. Xu, and B. Wang, "The physical and chemical characteristics of crude oil and oil-source of Juyanhai depression in Yingen-Ejina Basin," *Geological Bulletin of China*, vol. 39, no. 10, pp. 1589–1599, 2020.

[12] Z. Chen, W. Wang, and J. Liu, "Symbiotic characteristics and hydrocarbon accumulation mechanism of multi-type oil and gas reservoirs in the Hari sag, Yingen-Ejinaqi Basin," *Acta Sedimentologica Sinica*, vol. 40, no. 2, pp. 557–572, 2021.

[13] J. Y. Song, *Study on Sedimentary Facies and Four Characteristics of Reservoirs in Hari Sag, Yin'e Basin, [Ph.D. thesis]*, Northwest University, Xi'an, China, 2018.

[14] C. H. Zhijun, G. A. Yiwen, L. I. Huchuang et al., "Geochemical characteristics of lower cretaceous source rocks and oil-source correlation in Hari sag, Yingen-Ejinaqi Basin," *Acta Petrolei Sinica*, vol. 39, no. 1, pp. 69–81, 2018.

[15] L. Wu, "Analysis of complex rocks of Suhongtu formation in Hari sag, Yinhe Basin," *Ground Water*, vol. 40, no. 6, pp. 157-158, 2018.

[16] B. Chen, H. J. Gong, W. Z. Xue, and Z. H. Zhang, "Dolomite reservoirs in Hari sag of Yiner Basin," *Petroleum Geology and Engineering*, vol. 33, no. 3, pp. 17–21, 2019.

[17] H. Liu, W. Wang, Z. Chen, C. Zhao, B. Pan, and X. Bai, "Characteristics and accumulation conditions of cretaceous dolomitic mudstone gas reservoir in Hari sag, Yin'e basin," *Lithologic Reservoirs*, vol. 31, no. 2, pp. 24–34, 2019.

[18] X. D. Wang, L. Y. Ren, H. C. Liu et al., "Charcteristics and resource potential analysis of the lower cretaceous source rocks in the Hari sag, Yin/gen-Ejinaqi Basin," *Journal of Xi'An University of Science and Technology*, vol. 39, no. 2, pp. 286–293, 2019.

[19] X. Y. Bai, Y. H. He, X. F. Han, L. Y. Ren, F. X. Ma, and C. C. Han, "Identification Technology of Gray Mudstone gas Reservior in Hari sag of Yin'e Basio," *Northwestern Geology*, vol. 53, no. 2, pp. 270–279, 2020.

[20] Z. W. Wang and Z. J. Chen, "Recognition method of volcanic rocks in Hari sag, yine basin," *Petrochemical Technology*, vol. 27, no. 2, pp. 98-99, 2020.

[21] L. Y. Ren, Y. H. He, Z. J. Chen et al., "Fluid inclusion characteristics and hydrocarbon accumulation petrods of Bayingebi formation in Hari sag, the Yingen-Ejinaqi Basin," *China Petroleum Exploration*, vol. 24, no. 6, pp. 709–720, 2019.

[22] D. P. Hu, M. Lv, M. Q. Wang, and C. B. Fan, "Application of the X-ray diffraction analysis of the logging technology in Hari sag, Yin'e basin," *Journal of Baoji University of Arts and Sciences (Natural Science)*, vol. 40, no. 2, pp. 53–58, 2020.

[23] Y. L. Qiao, "Microscopic characteristics of carbonate mudstone reservoirs in Hani sag of Yiner Basin," *Petrochemical Technology*, vol. 27, no. 4, 2020.

[24] L. W. Zheng, S. N. Dong, S. L. Tang et al., "Clastic reservoir and micro-pore-throat characteristics of Bayinggobi Fornation in Hari sag," *Journal of Xi'An University of Science and Technology*, vol. 40, no. 2, pp. 304–313, 2020.

[25] T. T. Chang, Z. Zhang, W. H. Wang et al., "Hydrocarbon accumulation conditions and models of the Hari sag in the Yingen-Ejinaqi Basin," *Geology and Exploration*, vol. 58, no. 4, pp. 905–916, 2022.

[26] Z. J. Chen, F. X. Ma, G. Xiao et al., "Oil-sources rock correlation of Bayingebi formation in Hari sag, Yingen-Ejinaqi Basin," *Oil & Gas Geology*, vol. 40, no. 4, pp. 900–916, 2019.

[27] L. J. Lin, *Geochemical Characteristics of Mafic Volcanics and Discussion of Geotectonics Evolution from Carboniferous to Permian in Yin-E Basin, [Ph.D. thesis]*, Chang'an University, Xi'an, China, 2015.

[28] H. A. Zhang, J. D. Li, X. J. Wang et al., "Formation and evolution of Yin'gen-E'ji'naqi basin and propects for oil and gas exploration," *Petroleum Geology & Experiment*, vol. 42, no. 5, pp. 780–789, 2020.

[29] T. Wang, X. Han, H. Xu, X. Sun, T. Li, and Y. Hou, "Study on sedimentary facies based on unsupervised neural network seismic attribute clustering," *Oil Geophysical Prospecting*, vol. 56, no. 2, 2021.

[30] P. R. Vail, R. M. Mitchum, and S. I. Thompson, "Seismic stratigraphy and global changes of sea level: relative changes of sea level from coastal onlap," in *Seismic Stratigraphy–Applications to Hydrocarbon Exploration*, C. E. Payton, Ed., pp. 63–81, AAPG Memoir, Tulsa, OK, USA, 1977.

[31] P. R. Vail, "Seismic stratigraphy interpretation using sequence stratigraphy, part 1: seismic stratigraphy interpretation procedure," in *Atlas of Seismic Stratigraphy*, A. W. Bally, Ed., pp. 1–10, AAPG Studies in Geology, 1987.

[32] J. C. Van Wagoner, H. W. Posamentier, R. M. Mitchum et al., "An overview of the fundamentals of sequence stratigraphy and key definitions," in *Sea-level Changes: An Integrated Approach and Mineral*, vol. 42, pp. 39–45, Special Publication: Spring, 1988.

[33] O. Catuneanu, *Principles of Sequence Stratigraphy*, Amsterdam, UK, Elsevier, 2006.

[34] O. Catuneanu, V. Abreu, J. P. Bhattacharya et al., "Towards the standardization of sequence stratigraphy," *Earth Science Reviews*, vol. 92, no. 1-2, pp. 1–33, 2009.

[35] T. Kohonen, "Self-organized formation of topologically correct feature maps," *Biological Cybernetics*, vol. 43, no. 1, pp. 59–69, 1982.

[36] H. Simon, *Principle of Neural Network*, China Machine Press, Beijing, China, 2004.

[37] C. Y. Li, "Reflection shoot a realization of nerve Nerwork from the organization," *Computer Knowledge and Technology (Academic Exchange)*, vol. 21, 2007.

[38] J. Yu and P. Guo, "Research on self-organizing mapping (SOM) clustering algorithm," *Modern Computer*, vol. 3, 2007.

[39] X. Zhang, X. D. Zheng, J. S. Li, J. T. Lu, C. Y. Cao, and J. K. Sui, "Unsupervised seismic facies analysis technology based on SOM and PSO," *Chinese Journal of Geophysics*, vol. 58, no. 9, pp. 3412–3423, 2015.

[40] Y. G. Wang, D. Xie, Y. X. Le, and W. Liu, "Application of Sensmic attribute analysis technology in reservoir prediction," *Journal of the University of Petroleum China Natural Science Edition*, vol. 27, no. 3, 2003.

[41] A. R. Brown, *Interpretation of Three-dimensional Seismic Data*, AAPG Memoir 42, Tulsa, Oklahoma, 6th edition, 2004.

[42] X. Y. Yin and J. Y. Zhou, "Summary of optimum methods of seismic attributes," *Oil Geophysical Prospecting*, vol. 40, no. 4, 2005.

[43] S. Guo, Y. Chen, H. Yang et al., "Sedimentary facies analysis upon seismic attributes by K-means clustering algorithm in low-exploration areas: a case study of Wenchang formation in Baiyun Sag," *Marine Geology Frontiers*, vol. 34, no. 5, pp. 48–55, 2018.

[44] H. C. Jiao, *Study on Division Method of Seismic Facies in Three Seismic Data, [Ph.D. thesis]*, University of electronic science and technology of China, Chengdu, China, 2019.

[45] M. Z. Zhang, L. M. Ji, and S. Dai, "Climate Change Recorded by Early Cretaceous Sporo pollen in Yin'e Basin," in *Abstract of the 28th Annual Academic Conference of the Chinese Paleontological Society*, pp. 175-176, Shenyang, China, 2015.

[46] Y. M. Bai, H. J. Bo, W. L. Yang, C. Y. Li, Y. Yu, and Z. H. Tan, "Microfossils and Sedimentary Environment of the Lower Cretaceous Bayingobi Formation in Yigewusu Area, Ejin Banner, Yin'e Basin," *Geological Bulletin*, vol. 40, 2022.

[47] G. C. Chen, T. Jiang, J. Z. Shi, W. Li, H. Y. Zhang, and W. Han, "Late Paleozoic Sea level change and sedimentary response in Yin'e basin and adjacent areas in western Inner Mongolia," *Geological Bulletin*, vol. 31, no. 10, pp. 1645–1656, 2012.

[48] Y. Xiao, *Sequence Stratigraphy and Sedimentary Characteristics of Carboniferous Permian in Juyanhai Depression, Yin'e Basin*, China University of Petroleum, Beijing, China, 2019.

[49] R. Z. Yang, H. Y. Wang, T. L. Fan, Y. C. Hou, B. Zhang, and F. Zhang, "Structural characteristics of the Jiaozihu sag in Yin'e basin and its control on the evolution of paleogeomorphology," *Daqing Petroleum Geology and Development*, vol. 39, no. 6, pp. 39–51, 2020.

[50] Y. R. Guo, "Controlling factors and formation mechanism of closed lake basin sequence in Chagan fault depression of Yin'e basin," *Journal of Sedimentology*, vol. 31, no. 2, pp. 295–301, 2014.